

# STRONG MOTION MEASUREMENT USING SECURITY VIDEO CAMERAS

Muneo HORI<sup>1</sup>, Atsushi SUTOH<sup>2</sup> and Yoshihito SAITOH<sup>3</sup>

<sup>1</sup>Earthquake Research Institute, University of Tokyo (Yayoi, Bunkyo, Tokyo 113-0032, Japan)

<sup>2</sup>Technical R&D Department, Chizaki Co. (Nishi-Shinbashi, Minato, Tokyo 105-0003, Japan)

<sup>3</sup>Research Center, Maeda Co. (Asahimachi, Nerima, Tokyo 179-0032, Japan)

A dense network of strong motion measurement is significant for the earthquake hazard mitigation. To realize such a network, this paper proposes a strong motion measurement using video images recorded in security video cameras. Even though the accuracy is sacrificed to some extent, this measurement enables us to use video cameras as maintenance-free and simple apparatus which are installed in many buildings. The image analysis and the inversion are developed. Several tests were carried out to verify the validity of the methods, and it is shown that input acceleration can be fairly predicted from recorded video images.

**Key Words :** *strong motion measurement, image analysis, inversion, hazard mitigation*

## 1. INTRODUCTION

The significance of measuring the strong motion cannot be underestimated. Since Milne and Ewing first developed a seismograph, the technology of acquiring data in higher accuracy and a wider frequency range has been improved; see the review<sup>1)</sup> of the strong motion observation. For instance, a standard seismograph uses 32 bit data acquisition, and a new apparatus<sup>2)</sup> is aimed at using laser technology. Recently, various organizations<sup>3),4)</sup> are preparing a network of measuring the strong motion.

The strong motion measurement provides data used in various purposes. While the major purpose is for the inversion of an earthquake event, these data are used in earthquake engineering; information are extracted such that the nature of local quakes, such as the largest acceleration or velocity, are determined, and the form or spectra of input waves are investigated for the design purposes. Recently, these data have been being used for the hazard mitigation, as well as the urgent warning system<sup>5),6),7)</sup>.

On the view point of the hazard mitigation, it is desirable to clarify the nature of a local site in a finer length scale or to see the vibration characteristics of each structure. This is because the amplification of strong motion may vary depending on local ground conditions. A dense network of strong motion measurement is thus required. However, it is unrealistic to set advanced seismographs densely since initial and running costs are high. An alternative solution need to be found for the realization of such a network. The

solution requires a new method of measuring strong motion in a less expensive manner, even though the accuracy of measurement is sacrificed to some extent.

This paper examines the utilization of security video cameras as an apparatus of measuring strong motion. As will be discussed in the following section, video images record the relative movement of fixed objects due to the vibration of the camera or objects which move during earthquakes; see Appendix A for an example. While highest precision cannot be expected, there are three advantages for this strong motion measurement; 1) a huge number of security video cameras being used; 2) routine recording of data without extra equipment; and 3) less requirement for the maintenance of apparatus. The key issue of realizing the utilization of video cameras for the strong motion measurement is to develop analysis methods which extract strong motion data from video records with satisfactory accuracy. This paper proposes a pair of analysis methods, an image analysis of video records to capture strong motion effects appearing on records, and an inversion of the effects to evaluate the source strong motion.

## 2. STRONG MOTION MEASUREMENT

It should be first emphasized that the precision is sacrificed in measuring strong motion using a video camera. Furthermore, as most video cameras are located within buildings, the recorded strong motions influenced by the properties of the building as well as the soil-structure interaction (strictly speaking, video

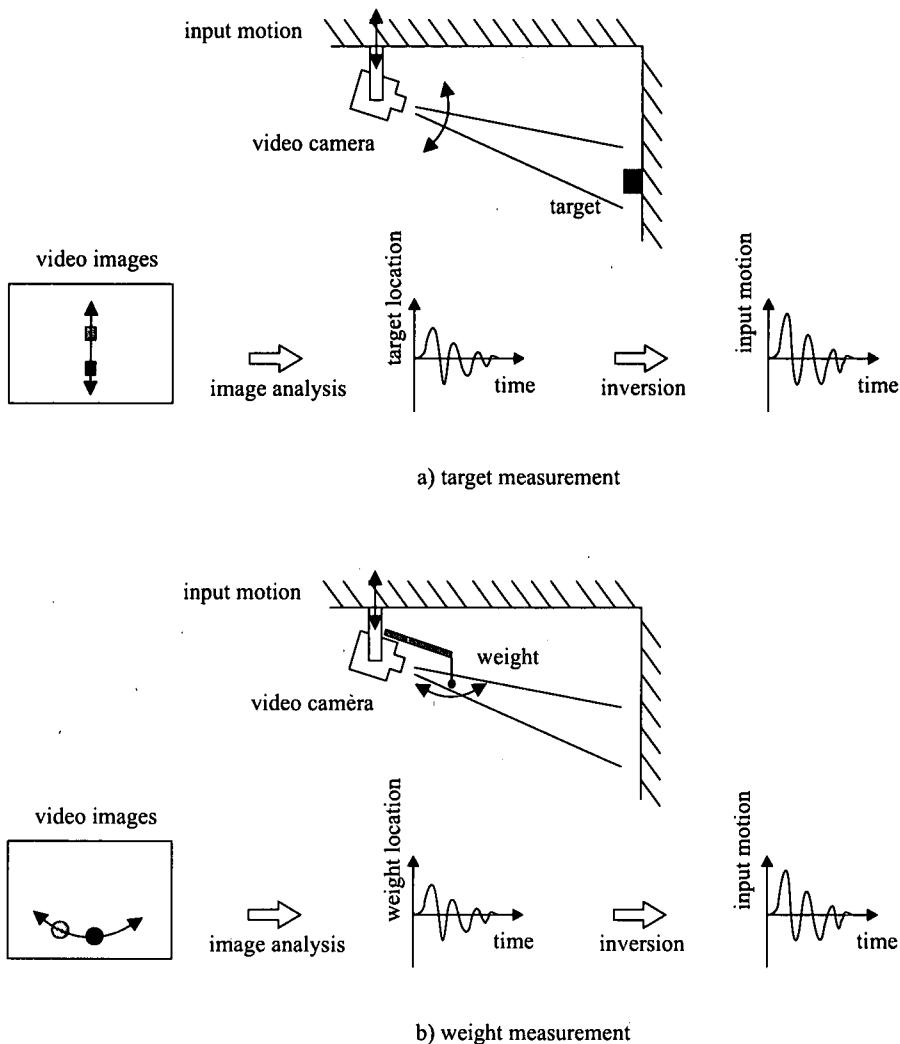


Fig. 1 Strategies of Strong Motion Measurement Using Video Camera

images record strong motion of a building, not strong motion of a ground). While such limitations are inevitable, placing an apparatus in high density has its own advantages; for each building or structure, data measured throughout long years can be used as for the health monitoring; the comparison of near-by sites can tell the relative strength of the strong motion in a smaller area; and it may be expected that data of huge amount can reveal hidden nature of the strong motion. Appendix B summarizes the advantage and disadvantages of the strong motion measurement using video cameras.

In this paper, we present two strategies<sup>8),9)</sup> to extract strong motion information from recorded images. The first strategy is the *target measurement*, which measures the vibration of a video camera through the relative movement of fixed objects in video image. No

special equipment is necessary, although the vibration characters of a camera or its attachment are known. The second strategy is the *weight measurement*, which chases the movement of some weights put to a video camera. The weights are two or three with suitably arranged natural frequencies, and must be small such that the security monitoring is not disturbed. **Figure 1** presents a schematic view of these two strategies. Another possibility is to attach a new device to video camera. For instance, small and less expensive transducers are a candidate; measured data on the acceleration are recorded on an audio track of a video tape. **Table 1** summarizes these three strategies.

The two strategies are aimed at measuring relatively large strong motion, say, of around three or five degrees. Smaller earthquakes may not cause enough movement of video cameras or weights, and too large

Table 1 Summary of Strategies

	strategy	advantages	disadvantages
1	target measurement	no special equipment is required	vibration character of camera and attachment must be known
2	weight measurement	accurate measurement is expected	suitable weight system must be attached
3	recording acceleration in audio track	most accurate measurement is possible	specially arranged video camera should be used

earthquakes may damage video cameras. In each city, relatively large earthquakes occur once a year or two, and the measurement using the video camera can be made more or less regularly; at least, each camera can yield quantitative information of the strong motion that happens to a building to which it is installed.

Since the hardware has little problem, the key issue is the software for the strong motion measurement using a video camera, i.e., to develop a method of extracting sufficiently accurate information of the strong motion from recorded video images. Best advantage should be taken of the recent advancement of the image analysis technology and the inversion techniques.

It should be mentioned that the measuring of strong motion using video images has been studied; Kikuchi<sup>10)</sup> used video images recorded in Hanshin Great Earthquake to measure movements of objects, and evaluated maximum acceleration; Ohori *et. al.*<sup>11)</sup> also used video images in a similar manner. While they did not apply the image analysis as considered here, they could extract some quantitative data from the video records.

### 3. FORMULATION

#### (1) Image Analysis

The image analysis is a technology which is most advanced in these decades, mainly owing to the development of computers; see the paper<sup>12)</sup> for a concise list of references. However, an ordinary image analysis may fail in analyzing the movement precisely, since strong motion does not produce large movement of objects in video images to be easily analyzed; for instance, when the movement is around 1% of the image size, it corresponds to just 5 pixels with an error of  $\pm 1$  pixels as one video image is discretized into  $640 \times 480$  pixels.

To overcome this shortcoming, we make use of whole recorded images; 300 data are obtained during 10[sec], since a video image is recorded every 1/30[sec] at the maximum. The accuracy of measuring the displacement can be increased by taking the regression<sup>12)</sup> with respect to time, if data of such a large number are used; see Fig. 2 for the schematic view of the re-

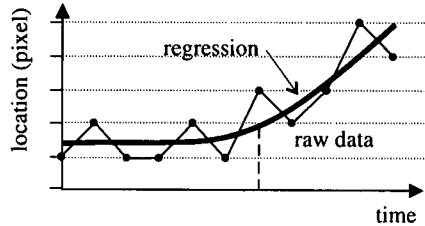


Fig. 2 Regression of Data of Large Number

Table 2 Results of Regression

$M$	1	2	3	$> 4$
$N$	5	10	15	$> 4M$

gression. Using a forth-order polynomial, the regression determines its coefficients such that the error of the polynomial and the data be minimized. Table 2 shows the results of numerical simulations which examines the minimum number of images ( $M$ ) in order to measure a given pixel number ( $N$ ) of the movement with the accuracy of 0.1 pixel unit. The regression works well provided that the motion is smooth.

It should be noted that while the spatial resolution can be increased, the strong motion of higher frequency (than, say, 8[Hz]) cannot be measured in video images as the recording is made every 1/30[sec]. Also, only one (or possibly two) component of displacement can be accurately extracted from video images; the direction of the component is in the plane of the recorded video image.

The increase of video images to be analyzed causes another problem. Provided that video records come from all sites in the network, huge amount of data need to be analyzed once a large earthquake takes place. The analysis of each video image must be as simple as possible. Hence, the binarization is applied to identify an object; the images are binarized to capture the location of the object center by specifying suitable threshold values of image data; see also Appendix A.

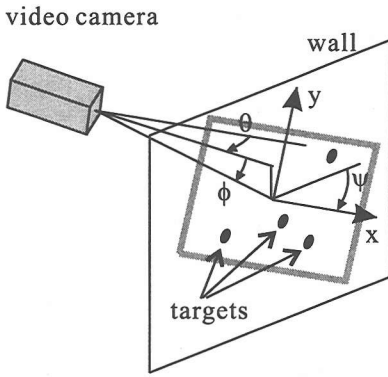


Fig. 3 Setting of Target Measurement

## (2) Inversion

First, we formulate the target measurement. Let  $(\theta, \phi, \psi)$  be the rolling, yawing, and pitching angles of a video camera located at  $d$  from a wall, and suppose that there are  $N$  objects on the wall; see Fig. 3. When an  $i$ -th object in the wall is viewed at the rolling and yawing angle  $(\theta_i, \phi_i)$ , it has the following coordinates,  $(x_i, y_i)$ , on a video image:

$$\begin{bmatrix} x_i \\ y_i \end{bmatrix} = d \begin{bmatrix} \cos \psi & -\sin \psi \\ \sin \psi & \cos \psi \end{bmatrix} \begin{bmatrix} \csc \theta - \csc \theta_i \\ \csc \phi - \csc \phi_i \end{bmatrix}. \quad (1)$$

As the camera vibrates,  $(\theta, \phi, \psi)$  varies and the fixed target appears to move. Therefore, measuring a time series of the location as  $(\bar{x}_i, \bar{y}_i)$  for each target, we can predict these angles such that the error function,  $E$ , is minimized,

$$E(\theta, \phi, \psi) = \sum_{i=1}^N (\bar{x}_i - x_i)^2 + (\bar{y}_i - y_i)^2. \quad (2)$$

While this error function is non-linear, finding the minimum is easy as  $(x_i, y_i)$ 's are explicitly given in Eq. (1).

Next, we formulate the weight measurement. It is assumed that the equation of motion for a weight is

$$m^\circ (\ddot{u}(t) + 2\alpha^\circ \dot{u}(t) + \beta^\circ u(t)) = m^\circ a(t), \quad (3)$$

where  $m^\circ$  is the mass and  $\alpha^\circ$  and  $\beta^\circ$  are constants; note that  $\omega^\circ = \sqrt{\beta^\circ - (\alpha^\circ)^2}$  is regarded as a natural angular frequency if  $\alpha^\circ$  is small, i.e.,  $\alpha^\circ \ll \sqrt{\beta^\circ}$ . These constants are easily determined by analyzing the free vibration of the weight. When  $u$  is measured at  $\Delta T$  interval and  $\{\bar{u}_i\}$  is a sequence of the measured displacement, the finite difference approximation of Eq. (3) leads to:

$$a_n = \frac{\bar{u}_{n+1} - 2\bar{u}_n + \bar{u}_{n-1}}{\Delta T^2}$$

Table 3 Shaking Table and Video Camera

shaking table	acceleration	0.01~100[gal]
	frequency	0.01~50[Hz]
video camera	pixel images	640×480[pixel]
	frame number	30[/sec]

Table 4 Input Motion

	H1	H2	H3
amplitude[gal]	30.0	30.0	30.0
frequency[Hz]	1.0	5.0	10.0

$$+ 2\alpha^\circ \frac{\bar{u}_{n+1} - \bar{u}_{n-1}}{2\Delta T} + \beta^\circ \bar{u}_n. \quad (4)$$

Here,  $a_n$  is the acceleration at the  $n$ -th step ( $n\Delta T$ ). It should be noted that two initial conditions are required to solve a differential equation of  $u$  for a given  $a$ , and the solution is obtained by integrating  $a$ . However, the inversion from  $u$  to  $a$  is straightforward as it requires only the differentiation of  $u$ .

While Eq. (4) is an exact discretization of Eq. (3), the evaluation of  $a$  may be poor because

1. components of frequencies much smaller or larger than  $\omega^\circ$  are almost filtered out;
2. the finite difference approximation of  $\ddot{u}$  can include larger errors.

To resolve these two problems, we take advantage of the following property of the governing equation, Eq. (3):

$$\begin{aligned} & \frac{1}{T} \int_0^T \exp(-\lambda^\circ t) a(\tau + t) dt \\ &= \frac{1}{T} [\exp(-\lambda^\circ t) (\dot{u}(\tau + t) + 2\alpha^\circ u(\tau + t))]_0^T. \end{aligned} \quad (5)$$

Here,  $\lambda^\circ$  is a complex-valued eigen-value of the left side, and the integration by part is used in deriving the right side of Eq. (5). As is seen, the integration of  $a$  is computed from  $\dot{u}$  and  $u$  only. For a sufficiently small  $T$ ,  $\exp(-\lambda^\circ t)$  is almost 1 and the left side of Eq. (5) is close to the average of  $a$ . Computing this weighted average for each weight and taking the sum, we can evaluate the input strong motion more accurately.

## 4. MODEL EXPERIMENTS

In order to examine the possibility of the strong motion measurement using a video camera, we first carried out model experiments to determine simple harmonic waves. A video camera was set on a computer-controlled shaking table; see Fig. 4. The properties of the shaking table and the video camera are summarized in Table 3, and the properties of the input harmonic are given in Table 4.

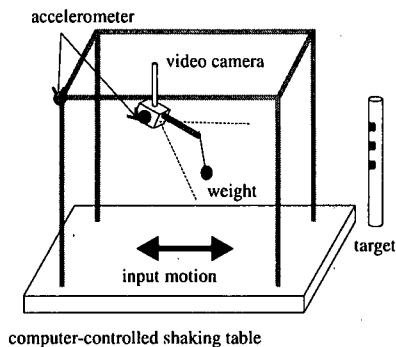


Fig. 4 Setting of Model Experiment

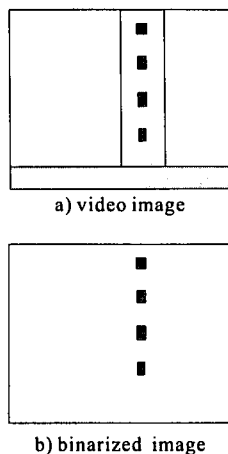


Fig. 5 Typical Images of Targets

For the target measurement, four markers of  $1 \times 1$  [cm] size were put on a pole and used as targets. The markers were green and vertically aligned on the pole. The pole faced the video camera in the right angle and stood in the distance of 1[m].

Figure 5 shows a schematic view of the targets; a) and b) are a video image and a binarized image, respectively. Note that all video images were binarized to capture the targets, by setting threshold values for the RGB values of the image which range 0 to 255 for each color; in the present case, the threshold values are (R,G,B)=(50,200,50).

Figure 6 plots the results of the image analysis. The horizontal movement of the four targets, which are obtained by analyzing 300 video images during 10[sec], are plotted with respect to time for the input wave of H1; see Table 4. Except for the presence of several spikes which are due to some noises in video tapes, a profile of harmonic waves are well captured. When the regression is made, the wave profile becomes smoother, and the analysis works satisfactorily. The

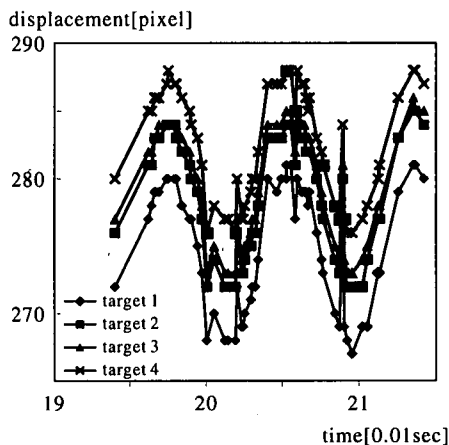


Fig. 6 Relative Movement of Targets

Table 5 Results of Target Measurement

harmonic	H1	H2	H3
amplitude[gal]	$34 \pm 5$	$25 \pm 5$	$26 \pm 5$
frequency[Hz]	$1.0 \pm 0.1$	$5.0 \pm 0.1$	$10.0 \pm 0.1$

inversion together with the image analysis can yield similarly good prediction for other harmonic waves (H2 and H3); Table 5 summarizes the predicted amplitude and phase. The analysis works satisfactorily as well as for sweep waves, in which the frequency of the input wave increases linearly with respect to the time.

For the weight measurement, three weights were used in experiments. The mass and the string of each weight were controlled such that the natural frequency ( $\omega^0/2\pi$ ) was 5.7, 6.1 and 7.5[1/sec]. The value of  $\alpha^0$  is of order of  $10^{-3}$ [1/sec] for all the three weights. The weights were attached to a small but stiff beam which was extended from the video camera.

Figure 7 shows typical video images of the weights. The weights have distinct color, red, silver, and yellow. Hence, it is easy to binarize the image to identify each weight, by setting particular threshold values as in the case of the target measurement.

Figure 8 plots the horizontal location of the weights for the input wave of H1. The image analysis leads to similar results for other waves; see Table 6 for the amplitude and frequency obtained from the inversion. The comparison of this table with Table 4 shows that the analysis can reproduce well the input wave properties.

As is seen, the properties of the input waves are well estimated by applying the proposed analyses. The relative error, the ratio of the predicted value to the exact one, is around 10%. Since the input waves are

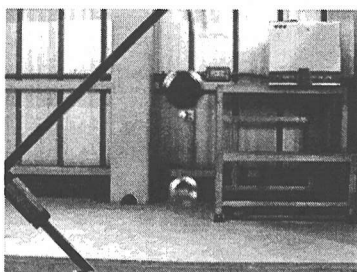


Fig. 7 Images of Weights

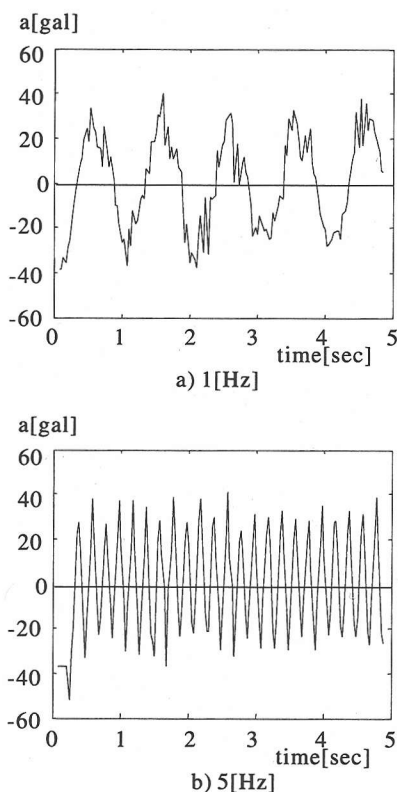


Fig. 8 Movement of Weights

Table 6 Results of Weight Measurement

harmonic	H1	H2	H3
amplitude[gal]	34±3	31±3	27±3
frequency[Hz]	1.0±0.1	5.0±0.1	10.0±0.1

simplest, such good prediction is not surprising. Still, it strongly supports the possibility of measuring strong motion using video images.

## 5. FURTHER TESTS

In order to examine the limitation of the strong motion measurement using a video camera, we carried out other tests. Random input accelerations were used for numerical simulation and model experiments.

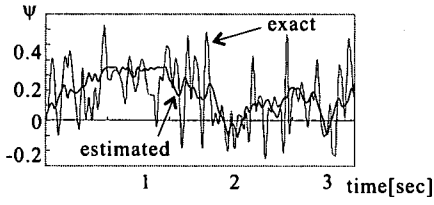
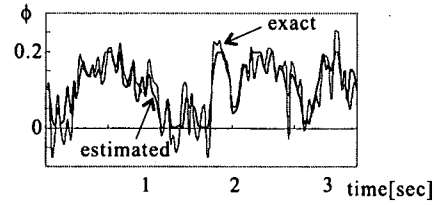
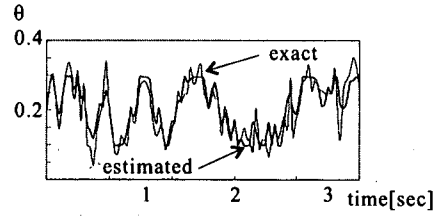
For the target measurement, we made the following numerical simulation: setting several targets on a wall, we first computed the change in their coordinates when a camera was vibrated due to a given acceleration. Then, we analyzed the camera vibration from the coordinates, putting some errors (10% of the exact values) in determining them; see Fig. 3. The time change of  $(\theta, \phi, \psi)$ , together with the input values, are plotted in Fig. 9; a) and b) are for cases when three and ten targets were used. As is seen, the prediction is successful.

It is shown that even if the image analysis poorly identify the coordinate, the inversion of  $(\theta, \phi, \psi)$  can be made by using targets of a larger number. As mentioned, it is easy to find the minimum of the non-linear error function,  $E$  given by Eq. (2). However, a coordinate change must be larger than 1[pixel] for targets far from the camera, such that the inversion is reliable. Hence, the target measurement is applied to an earthquake which causes a sufficiently large vibration of a vide camera.

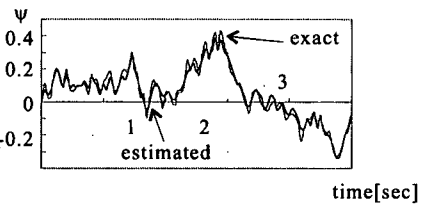
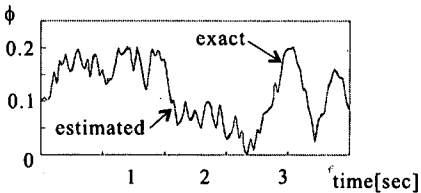
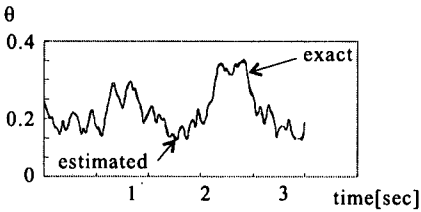
For the weight measurement, we carried out other model experiments which used random accelerations. The results of the inversion using Eq. (4) are presented in Fig. 10; a), b), and c) are for weights of  $\omega^\circ = 36.2, 37.9$ , and  $47.3$  [sec], respectively, and d) is the in-site acceleration measured by a transducer. While the analyzed accelerations are of the same order as the exact one, the profiles are different. Changing the amplitude of the input acceleration with the phase being fixed, we made other experiments and then compute the inversion. The computed maximum accelerations are plotted in Fig. 11; the average of the three accelerations is also plotted. The prediction is satisfactory with relative error of 10%.

While overall profiles of the inverted acceleration are fairly similar to the measured one, the local profiles are quite different as mentioned. This is due to a high natural frequency ( $\omega^\circ/2\pi > 10$ [Hz]) of the weight; Fig. 12a) and b) show typical examples of analyzed displacement ( $u$ ) and acceleration ( $a$ ).

When weights of slower natural frequencies ( $\omega^\circ/2\pi = 1.4, 1.7, 2.0$  [sec]) are used, we can measure smoother wave profiles; Fig. 13 shows an example of the inversion for a weight of  $\omega^\circ = 1.4$  [sec]. Due to the filtering of the natural frequencies, the inversion fails as the analyzed acceleration is smaller by one order. Instead of Eq. (4), we use Eq. (5) and take the sum of the weighted accelerations; Fig. 14a)



a) 3 targets



b) 10 targets

Fig. 9 Change in  $(\theta, \phi, \psi)$

and b) show the weighted displacement and the sum of the three accelerations, respectively. As is seen, the wave become much smoother, and this treatment can produce the change of  $a$  accurately.

As is seen in Fig. 11, a parameter such as the maximum acceleration can be predicted by using the results of the inversion, even though the inversion fails

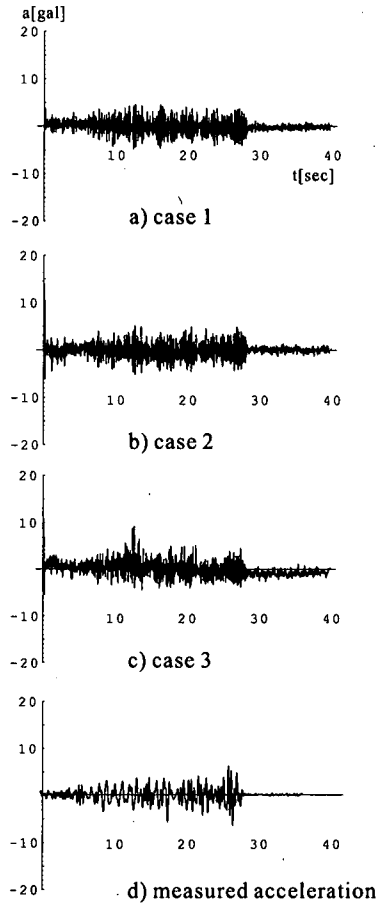


Fig. 10 Inverted Acceleration (1)

in identifying wave profiles (Fig. 10). This is because each weight catches waves in a narrow frequency range. To show this, Fig. 15 plots the change in the amplitude and phase,  $A$  and  $\theta$ , for a weight of  $\omega^0/2\pi = 1.4[\text{Hz}]$ ; the amplitude and phase are computed by applying the following local Fourier transform:

$$A \exp(i\theta) = \frac{2}{T^0} \int_0^{T^0} \exp(i\omega^0 t) u(t) dt, \quad (6)$$

where  $T^0 = 2\pi/\omega^0$ . It is shown that  $\theta$  changes almost linearly, which means that a component near the natural frequency is dominant. Other weights have a similar linear change in the phase, although the change in the amplitude is different; see Fig. 16.

While a weight of large damping effects catches waves of wider frequency range, the amplitude is decreased accordingly. This trade-off, i.e., a smaller amplitude or a narrower frequency range, is inevitable when weights of slower natural frequency are used. The maximum acceleration, however, can be predicted in the same accuracy as shown in Fig. 11. Since the

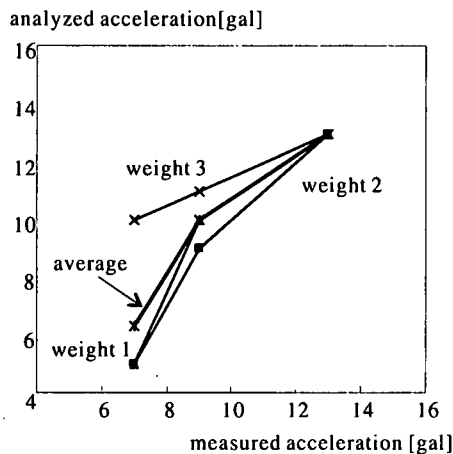


Fig. 11 Inverted Maximum Acceleration

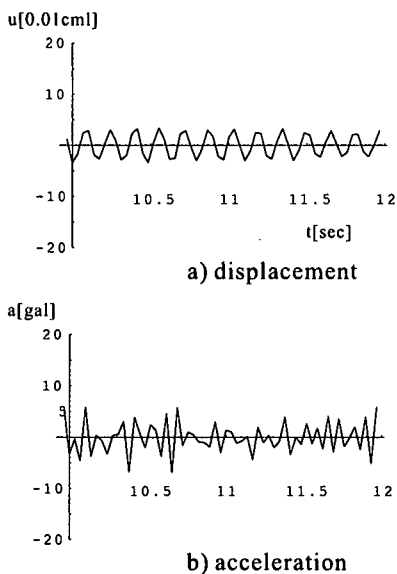


Fig. 12 Local Profile of  $u$  and  $a$

amplitude of  $u$  becomes larger as  $\omega^0$  becomes smaller, weights of smaller natural frequencies may be suitable in measuring such quantity instead of the wave profile.

## 6. CONCLUDING REMARKS

Two strategies are proposed for the strong motion measurement using a video camera. The results of several tests support the possibility of this measurement, even though the accuracy in identifying input acceleration could be improved. Still, there remain several technical difficulties, such as the interpretation of the measured acceleration that is filtered through the vi-

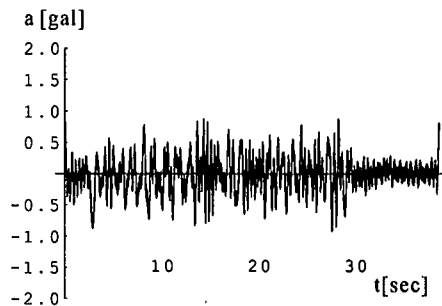


Fig. 13 Inverted Acceleration (2)

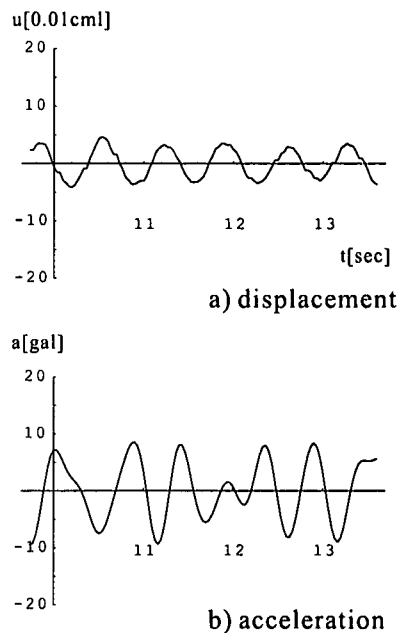


Fig. 14 Averaged and Summed  $a$

bration characteristics of buildings to which the camera is installed. Furthermore, more simple analysis will be needed as the number of available cameras is huge in densely populated cities. We are now carrying out an experiment which uses actual security video cameras; the validity and usefulness are examined as these video cameras are located close to a seismometer.

The third strategy is a candidate for the strong motion measurement with more accuracy. As briefly mentioned, the implementation of a transducer to a video camera is promising in measuring the strong motion much more accurately. Preliminary experiments show the potential usefulness of this measurement method.



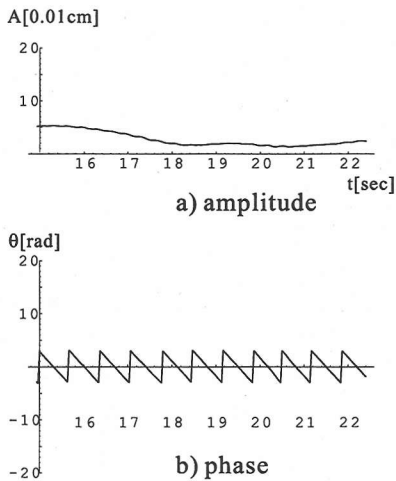


Fig. 15 Amplitude and Phase Change

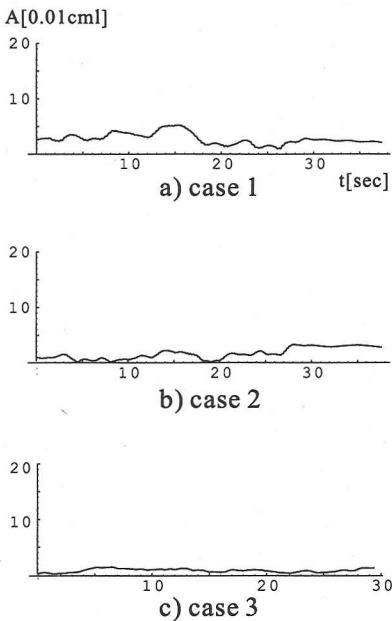


Fig. 16 Amplitude Change of Three Weights

## APPENDIX A VIDEO ANALYSIS

As an illustrative example, we present the image analysis of actual video images; the images were recorded by NHK<sup>13)</sup> during the Great Hanshin Earthquake. The target is a clock on the wall; see Fig. 17. The results of the image analysis are shown in Fig. 18. In this analysis, we apply the pattern matching to identify the clock, which takes a longer computation than the binarization that is used in the present paper. Both the horizontal and vertical coordinates are plot-

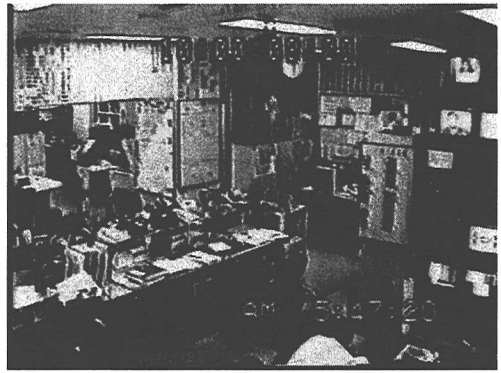


Fig. 17 Examples of Video Images

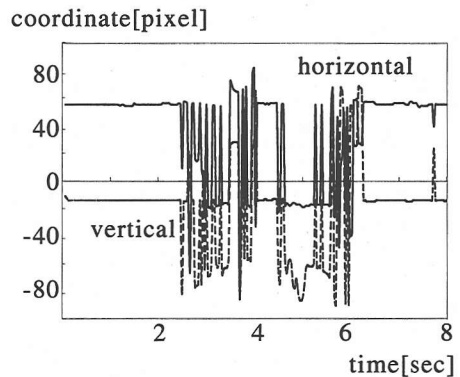


Fig. 18 Change in Target Coordinate

ted with respect to the time, and some sudden changes of the coordinates are caused by the movement of the camera. Possible acceleration can be estimated from such coordinate changes, though the estimate is not made in this paper.

## APPENDIX B ADVANTAGES

As an apparatus used in a network of strong motion measurement, security video cameras have the following advantages:

1. dense network: Security video cameras are located in most of banks and shops, and a denser network is being naturally formed in a largely populated area.
2. routine recording: Video images, each of which contains, say,  $640 \times 480$  pixel data in each  $1/30[\text{sec}]$ , are recorded while the banks and shops are open.
3. easy maintenance: No special maintenance of apparatuses is required, and video cameras are regularly maintained for its primary function of security watching.

## REFERENCES

- 1) Kudo, K.: Strong earthquake motion observation - Present status and Prospects -, *Jishin 2*, Vol. 47, pp. 225-237 (1994, in Japanese).
- 2) Araya, A., Kawabe, K., Sato, T., Mio, N. and Tsubono, K.: Highly sensitive wideband seismometer using a laser interferometer, *Rev. Sci. Instrum.*, Vol. 64, No. 5 pp. 1337-1341 (1993).
- 3) Kyoshin Net (<http://www.k-net.bosai.go.jp/>)
- 4) City of Yokohama, Dense Network of Strong Motion Measurement (<http://www.city.yokohama.jp/me/bousai/eq/>)
- 5) Nakamura, Y. and Ueno, M.: Development of UREDAS for urgent warning system of earthquakes, *Proc. of 7th Earthquake Eng.*, pp. 2095-2100 (1986, in Japanese).
- 6) Shimizu, Y.: SIGNAL for urgent prediction system of earthquake damage, *Measurement and Control*, Vol. 36, pp. 41-44 (1997, in Japanese).
- 7) Yamazaki, F.: Review on the development of earthquake monitoring and early damage assessment system in Japan, *J. Struct. Mech. Earthquake Eng.*, JSCE, No. 577/I-41, pp. 1-16 (1997, in Japanese).
- 8) Saitoh, Y., Hori, M. and Sutoh, A.: Possibility of security cameras as strong motion measurement system, *Proc. of 24th Earthquake Eng. Sympo.* (1997, in Japanese).
- 9) Sutoh, A., Hori, M. and Saitoh, Y.: Shaking table experiments for strong motion measurement using image analysis, *Proc. of 24th Earthquake Eng. Sympo.* (1997, in Japanese).
- 10) Kikuchi, M.: Read video images of strong motion, *Kagaku*, Vol. 65, pp. 569-572 (1995, in Japanese).
- 11) Ohori, M., Okuda, A., Wakamatsu, K. and Yasui, Y.: Hokkaido-Toho-Oki Earthquake on October 4, 1994 recorded by security cameras at convenience stores, *Jishin 2*, Vol. 48, pp. 423-427 (1995, in Japanese).
- 12) Adachi, S., Gotho, H. and Hori, M.: Inversion of stress-strain relation of geo-textile ground mold using video camera records, *Proc. of 31th Geoenvironment*, pp. 15-16 (1997, in Japanese).
- 13) courtesy of Prof. Kikuchi (Earthquake Research Institute, University of Tokyo, 1997).

(Received May 1, 1999)

## 防犯用ビデオカメラを用いた強震動測定

堀 宗朗・須藤敦史・斎藤芳人

高密度強震動測定のために、防犯用ビデオカメラを用いた強震動の測定方法を提案する。測定精度はある程度犠牲にするものの、ビデオカメラは簡便で管理が容易な計測装置として利用できる。測定方法はビデオ画像の画像解析と逆解析に基づくものであり、画像内の物体の動きをとらえ、その動きを引き起こした入力加速度を計算する。モデル実験等を行い二つの解析の妥当性を検討したところ、入力加速度を評価しうることが示された。これは提案された測定方法の可能性を裏付けるものである。